Sensors & Transducers, Vol. 27, Special Issue, May 2014, pp. 295-298

www.sensorsportal.com

Sensors & Transducers

http://www.sensorsportal.com

Synthesis and Luminescence Properties of Yellow-emitting SiO_2/Zn_2SiO_4:Mn Nanocomposite

[1, 2] Karim OMRI, [1, 2] Lassaad EL MIR, [1] Hassen DAHMAN and [3] Carlos BARTHOU

[1] Laboratoire de Physique des Matériaux et des Nanomatériaux Appliquée à l'Environnement, Faculté des Sciences de Gabès, Cité Erriadh Manara Zrig 6072 Gabès, Tunisia

[2] Al Imam Mohammad Ibn Saud Islamic University (IMSIU), College of Sciences, Department of Physics, Riyadh 11623, Saudi Arabia

[3] Institut des NanoSciences de Paris (INSP), UPMC Université Paris 6, CNRS UMR 7588, 140 rue de Lourmel - F-75015 Paris France

[1] Tel.: +21697276251, fax: +21675392421

[1] E-mail: Lassaad.ElMir@fsg.rnu.tn

Received: 23 November 2013 /Accepted: 12 January 2014 /Published: 26 May 2014

Abstract: Yellow light emitting Mn^{2+}–doped β–Zn_2SiO_4 phosphor nanoparticles embedded in SiO_2 host matrix, were prepared by a simple solid-phase reaction under natural atmosphere at 1500 °C for 2 hours after the incorporation of manganese doped zinc oxide nanoparticles in silica using sol-gel method. The SiO_2/Zn_2SiO_4:Mn nanocomposite was characterized by X-ray diffraction (XRD), transmission electron microscopy (TEM), scanning electron microscopy (SEM) and photoluminescence (PL). The nanopowder was crystallized in triclinic β–Zn_2SiO_4 phase with a particles size varies between 70 nm and 84 nm. The SiO_2/β–Zn_2SiO_4:Mn nanocomposite exhibited a broad yellow emission band at 575 nm under UV excitation light. The dependence of the intensity and energy position of the obtained PL band on measurement temperature and power excitation will be discussed. *Copyright © 2014 IFSA Publishing, S. L.*

Keywords: Zn_2SiO_4, Zinc Oxide, Nanoparticles, Sol-gel, Optical Materials.

1. Introduction

Nanoparticles have recently been recognized tremendous potential in the area of photonic applications [1]. Combining the promising optical properties of transition metal (TM) ions and nanoparticles, the study of excited state dynamics of TM ions in nanoscale environment is important. In case of transition metals ions, the electronic d–d transitions involve electrons which are localized in atomic orbitals of the ions. The host lattice of Zn_2SiO_4 containing Eu^{3+}, Mn^{2+} or Ce^{3+} dopant ions covers the red, green, and blue portions of the visible spectrum, respectively [2–4]. The emissions bands at 525 nm (α-Zn_2SiO_4:Mn) and 576 nm (β-Zn_2SiO_4:Mn) are due to the spin-forbidden ^4T_1g–^6A_1g transition of the $3d^5$ electronic configuration of isolated Mn^{2+} [5]. Among polymorphic zinc silicate, the α-phase appears to be the stable form, while the β-phase is metastable and can only occur under a certain condition [6]. For examples, Mai and Feldmann [7] synthesized Mn doped β-Zn_2SiO_4 by melting and rapidly cooling mixtures of Zn_2SiO_4 composition from 750 °C. Taghavinia et al. [8] grew β-Zn_2SiO_4 particles inside oxidized porous silicon by annealing zinc and manganese salts up to 1050 °C for 30 min as a major product, but α-Zn_2SiO_4 becomes dominate phase by increasing the annealing time to more than 15 h [9–11].

In this paper, we report a novel sol–gel process to synthesize nanosized of ZnO:Mn and SiO_2/Zn_2SiO_4:Mn nanocomposite. However, the optical and structural properties of this SiO_2/β-Zn_2SiO_4:Mn^{2+} nanocomposite was not studied in detail. Here we report how to synthesize yellow-emitting, in an easy and reproducible way, and will identify the source of luminescence. The in-situ synthesize used process give the sample more stability in time.

2. Experimental Details

2.1. Synthesis Process of SiO_2/Zn_2SiO_4:Mn Nanocomposites

The samples were prepared by a sol–gel method based on L. El Mir et al. protocol [12-14]. In the first step, nanoparticles aerogel were obtained by supercritical drying in ethyl alcohol (EtOH). In the second step, we have prepared ZnO:Mn confined in aerogel according to the following process: 0.5 ml of TEOS was first dissolved in EtOH. Then, with constant stirring of the mixture of TEOS and EtOH, 0.44 ml of water and 30 mg of ZnO:Mn powder prepared in the first step was added. The whole solution was stirred for about 30 min, resulting in the formation of a uniform sol. The sol was transferred to tube in an ultrasonic bath where 100 µl of fluoride acid was added. The wet gel was formed in a few seconds. Monolithic and transparent aerogel was obtained by supercritical drying in EtOH as described in the first step. Finally, silica glasses containing ZnO:Mn and Zn_2SiO_4 particles were obtained after firing the aerogel at high temperature. The aerogel was put into a furnace and heated up to the densification temperature at a heating rate of 50 °C/h. After this step, we performed a heat treatment in air at 1500 °C for two hours in order to obtain the SiO_2/β-Zn_2SiO_4:Mn nanocomposites. The densification temperature selected (1500 °C), was still lower than the fusion temperature of glasses, and the formation of macro-fissures did not occur. The density achieved at increasing temperature shows two transitions: the first one situated near 700 °C was attributed to the disappearance of the micropores and small mesopores in the aerogel whereas the second one located at 1200 °C was attributed to the final densification to glass with a density of about 2 [15].

2.2. Characterization

The crystalline phases of annealed powders were identified by X-ray diffraction (XRD) using a Bruker D5005 powder X-ray diffractometer using a CoKα source (1.78901 Å radiation). Crystallite sizes (G, in Å) were estimated from the Scherrer's equation [16]:

$$G = \frac{0.9\lambda}{B\cos\theta_B}, \quad (1)$$

where λ is the X-ray wavelength (1.78901 Å), θ_B is the maximum of the Bragg diffraction peak (in radians) and B is the linewidth at half maximum.

Scanning electron microscope (SEM, JEOL JSM-6300) and transmission electron microscopy (TEM, JEM-200CX) were used to study the morphology and particle size of the phosphor powders. The specimens for TEM were prepared by putting the as-grown products in EtOH and immersing them in an ultrasonic bath for 15 min, then dropping a few drops of the resulting suspension containing the synthesized materials onto TEM grid.

The measurements of photoluminescent excitation and emission spectra, as well as temperature-dependent PL spectra of the nanocomposites, were analyzed out using a Jobin-Yvon Spectrometer HR460 and a multichannel CCD detector (2000 pixels), equipped with a 450-W Xenon lamp as the excitation light source. The low temperature experiments were carried out in a Janis VPF-600 Dewar with variable temperature controlled between 78 K and 300 K.

3. Results and Discussions

3.1. Structural Studies

Fig. 1 shows the XRD patterns of SiO_2/β–Zn_2SiO_4:Mn nanocomposite synthesized by sol-gel process. It is found that the sample is indexed to triclinic symmetry, such as the lattice parameters are $a = 5.09$ Å, $b = 9.95$ Å and $c = 15.89$ Å, these lattice parameter are very close to β-Zn_2SiO_4 ones, i.e., $a = 5.1$ Å, $b = 9.94$ Å and $c = 15.9$ Å [7,17,18].

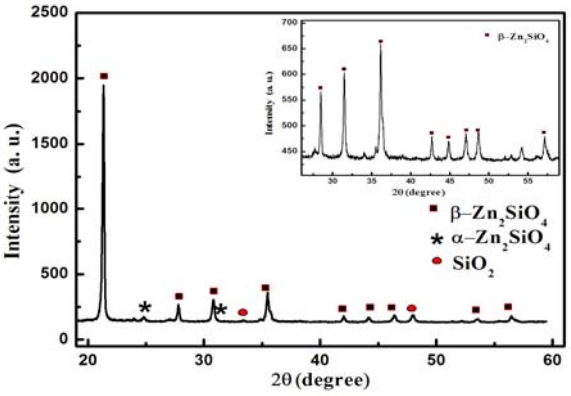

Fig. 1. X-ray diffraction pattern of the SiO_2/β–Zn_2SiO_4:Mn nanocomposite.

We can clearly see the existence a single phase of β–Zn_2SiO_4 (JCPDS No. 19-1479) [7] at high temperature (1500 °C), where the XRD intensity of the sample is high because of its high crystallinity. Nevertheless, the correspondence is enough to claim that it is a β–phase. The pattern represents only one

phase, demonstrating that the sample comprises β–Zn_2SiO_4 particles embedded in a silica matrix. The result further confirms that Zn^{2+} ions can be replaced by Mn^{2+} ions within zinc silicate lattice in large scale of molar ratio due to their similar ionic radii (0.80 Å for Mn^{2+} and 0.74 Å for Zn^{2+}). Like previously, according to the Scherrer formula (1), we found the sizes of nanoparticles for both nanocomposites β–Zn_2SiO_4, vary between 70 and 80 nm [15].

SEM (Fig. 2) and TEM (Fig. 3) observations show that very small β–Zn_2SiO_4:Mn particles are present in the as-prepared nanocomposite. The size of the majority of β–Zn_2SiO_4:Mn particles in this powder varied between 75 and 90 nm [7, 15]. Taking into account the results of crystallite size measurements by XRD, it can be concluded that the crystallite size is approximately equal to the particle size in β–Zn_2SiO_4:Mn powder prepared in the present work.

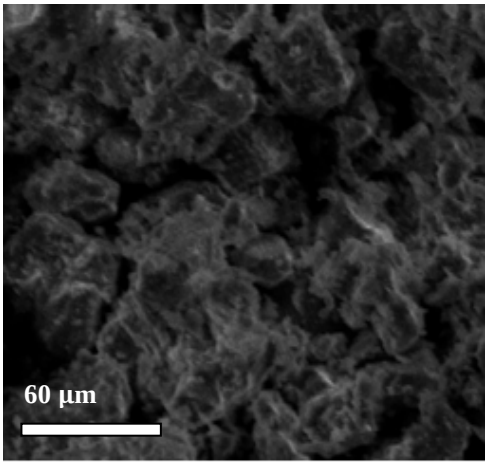

Fig. 2. SEM photograph showing the general morphology of the SiO_2/β–Zn_2SiO_4:Mn nanocomposite.

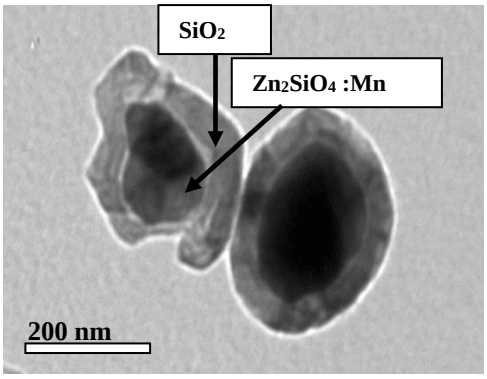

Fig. 3. TEM photograph showing the general morphology of the SiO_2/β–Zn_2SiO_4:Mn nanocomposite.

3.2. Optical Properties

Fig. 4. shows the typical PL spectra of SiO_2/β–Zn_2SiO_4:Mn nanocomposite prepared at 1500 °C for 2 h. The yellow emission spectra in Fig. 4 excited by 255 nm agree well with the literature value which has been assigned to an electronic transition of $^4T_1(^4G) \rightarrow {}^6A_1(^6S)$ peaking around the wavelength of 575 nm and which is a parity forbidden emission transition of Mn^{2+} ions [8, 17, 18]. Fig. 5 shows the excitation spectra of the SiO_2/β–Zn_2SiO_4:Mn nanocomposite measured for 575 nm emission.

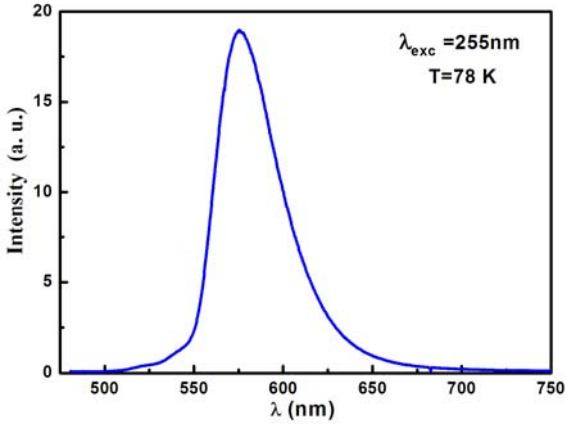

Fig. 4. PL spectrum of a typical SiO_2/β–Zn_2SiO_4:Mn nanocomposite.

The excitation spectrum shows an excitation band ranging from 220 to 300 nm with a maximum at around 255 nm, which mainly corresponds to charge transfer transition (or the ionization of manganese) from the divalent manganese ground state (Mn^{2+}) to the conduction band (CB) [8,18].

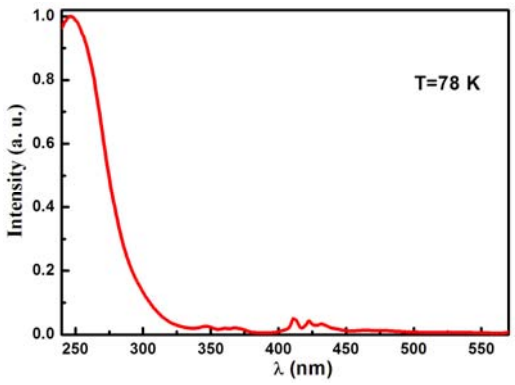

Fig. 5. PLE spectrum of a typical SiO_2/β–Zn_2SiO_4:Mn nanocomposite.

The tendency of excitation intensity is similar to that of emission as seen in Fig. 4, thus the most efficient excitation of charge transfer leads to the maximum emission intensity. The radiative transition in the β–phase corresponds to $^4T_1 \rightarrow {}^6A_1$ transition in Mn ion. Increasing the crystal field is known to shift the emission of Mn^{2+} towards longer wavelengths [8].

This implies that Mn ions in β-phase feel a stronger crystal field. We do not know whether this effect is a result of shorter Mn–O bonds or is related to the difference in the coordination number. It should be noted that the yellow emission of SiO_2/β–Zn_2SiO_4:Mn nanocomposite synthesized by the sol-gel process is based on the $^4T_1(^4G)\rightarrow{}^6A_1(^6S)$ transition of $3d^5$ electrons in the Mn^{2+} ion, which is the same as that for material synthesized by the solid-state reaction process [17].

4. Conclusions

Yellow light emitting SiO_2/β–Zn_2SiO_4:Mn nanocomposite was produced using a slightly modified version of the conventional sol-gel method used to synthesize silica aerogels reached by nanoparticles. The nanocomposite materials had monolithic structures with well dispersed luminescent nanoparticles in silica network. The X-ray diffraction, SEM and TEM show a crystalline phase β–Zn_2SiO_4 with a particle size ranging between 75 and 80 nm. The addition of manganese enhanced the crystallization of β–Zn_2SiO_4:Mn crystals. The PL spectrum of our Mn^{2+} doped β–Zn_2SiO_4 phosphor particles, under UV irradiation at 255 nm is shown a emission located at 575 nm, attributable to the $^4T_1(^4G)\rightarrow{}^6A_1(^6S)$ transition in Mn^{2+} doping centers.

References

[1]. R N. Bhargava, D. Gallaghar, X. Hong, A. Nurmikko. Optical properties of manganese-doped nanocrystals of ZnS, *J. Phys. Rev. Lett.* Vol. 72, Issue 2, 1994, pp. 416-419.

[2]. J. Park, K. Park, S. Lee, J. Kim, G. Kim, J. Yoo, A simple synthesis method for Zn_2SiO_4:Mn^{2+} phosphor films and their optical and luminescence properties. *J. Luminescence*, Vol. 134, 2013, pp. 71-74.

[3]. C. Barthou, J. Benoit, P. Benalloul, A. Morell. Mn^{2+} Concentration Effect on the Optical Properties of Zn_2SiO_4: Mn Phosphors, *J. Electrochem. Soc.,* Vol. 141, 1994, pp. 524-528.

[4]. Q. Y. Zhang, K. Pita, W. Ye, W. X. Que, Influence of annealing atmosphere and temperature on photoluminescence of Tb^{3+} or Eu^{3+}-activated zinc silicate thin film phosphors via sol–gel method, *Chem. Phys. Lett.,* Vol. 351, 2000, pp. 163-170.

[5]. Z. Li, H. Zhang, H. Fu, Facile synthesis and morphology control of Zn_2SiO_4:Mn nanophosphors using mesoporous silica nanoparticles as templates, *J. Luminescence*, Vol. 135, 2013, pp. 79-83.

[6]. H. F. W. Taylor. The dehydration of hemimorphite, *J. Am. Mineral.* Vol. 47, 1962, pp. 932.

[7]. M. Mai, C. Feldmann, Two-color emission of Zn_2SiO_4:Mn from ionic liquid mediated synthesis, *J. Solid State Sciences*, Vol. 11, Issue 2, 2009, pp. 528–532.

[8]. N. Taghavinia, G. Lerondel, H. Makino, A. Yamanoto, T. Yao, Y. Kawazoe, T. Goto, Growth of luminescent Zn_2SiO_4:Mn^{2+} particles inside oxidized porous silicon: emergence of yellow luminescence, *J. Cryst. Grow.,* Vol. 237, 2002, pp. 869-873.

[9]. J. Wan, Z. Wang, X. Chen, L. Mu, W. Yu, Y. Qian, Controlled synthesis and relationship between luminescent properties and shape/crystal structure of Zn_2SiO_4:Mn^{2+} phosphor, *J. Luminescence,* Vol. 121, 2006, pp. 32-38.

[10]. N. Taghavinia, G. Lerondela, H. Makino, A. Parisini, A. Yamamoto, T. Yao, Y. Kawazoe, T. Goto, Activation of porous silicon layers using Zn_2SiO_4:Mn^{2+} phosphor particles, *J. Luminescence*, Vol. 96, 2002 pp. 171–175.

[11]. V. Sivakumar, A. Lakshmanan, S. Kalpana, R. S. Rani, R. S. Kumar, M. T. Jose. Low-temperature synthesis of Zn_2SiO_4:Mn green photoluminescence phosphor, *J. Luminescence*, Vol. 132, 2012, pp. 1917–1920.

[12]. L. El Mir, Z. Ben Ayadi, H. Rahmouni, J. El Ghoul, K. Djessas, H. J. von Bardeleben. Elaboration and characterization of Co doped, conductive ZnO thin films deposited by radio-frequency magnetron sputtering at room temperature, *Thin Solid Films*, Vol. 517, Issue 2, 2009, pp. 6007-6011.

[13]. L. El Mir, A. Amlouk, C. Barthou, S. Alaya, Synthesis and luminescence properties of ZnO/Zn_2SiO_4/SiO_2 composite based on nanosized zinc oxide-confined silica aerogels, *J. Physica B*, Vol. 388, Issues 1–2, 2007, pp. 412-417.

[14]. L. El Mir, Z. Ben Ayadi, M. Saadoun, K. Djessas, H. J. Von Bardeleben, S. Alaya. Preparation and characterization of n-type conductive (Al, Co) co-doped ZnO thin films deposited by sputtering from aerogel nanopowders, *Appl. Surf. Sci.* Vol. 254, Issue 2, 2007, pp. 570-573.

[15]. J. El Ghoul, K. Omri, L. El Mir, C. Barthou, S. Alaya. Sol–gel synthesis and luminescent properties of SiO_2/Zn_2SiO_4 and SiO_2/Zn_2SiO_4:V composite materials, *J. Luminescence*, Vol. 132, Issue 9, 2012, pp. 2288-2292.

[16]. J. El Ghoul, C. Barthou, L. El Mir. Synthesis by sol–gel process, structural and optical properties of nanoparticles of zinc oxide doped vanadium, *J. Superlattices and Microstructures*, Vol. 51, Issue 6, 2012, pp. 942-951.

[17]. Y. Jiang, J. Chen, Z. Xie, L. Zheng. Syntheses and optical properties of α- and β-Zn_2SiO_4:Mn nanoparticles by solvothermal method in ethylene glycol–water system, *J. Materials Chemistry and Physics*, Vol. 120, 2010, pp. 313-318.

[18]. M. Takesue, H. Hayashi, R. Lee Smith, Thermal and chemical methods for producing zinc silicate (willemite): A review, *J. Progress in Crystal Growth and Characterization of Materials*, Vol. 55, 2009, pp. 98-124.